ISSN 0040-5795, Theoretical Foundations of Chemical Engineering, 2013, Vol. 47, No. 5, pp. 524–537. © Pleiades Publishing, Ltd., 2013.
Original Russian Text © V.A. Kirillov, A.B. Shigarov, N.A. Kuzin, V.V. Kireenkov, Yu.I. Amosov, A.V. Samoilov, V.A. Burtsev, 2013, published in Teoreticheskie Osnovy Khimicheskoi Tekhnologii, 2013, Vol. 47, No. 5, pp. 503–517.

Thermochemical Conversion of Fuels into Hydrogen-Containing Gas Using Recuperative Heat of Internal Combustion Engines

V. A. Kirillov[a, b,*], A. B. Shigarov[a, b], N. A. Kuzin[a, b], V. V. Kireenkov[a, b], Yu. I. Amosov[a, b], A. V. Samoilov[a, b], and V. A. Burtsev[c]

[a] *Boreskov Institute of Catalysis, Siberian Branch of Russian Academy of Sciences, pr. Akademika Lavrent'eva 5, Novosibirsk, 630090 Russia*
[b] *"UNICAT Ltd." pr. Akademika Lavrent'eva 5, Novosibirsk, 630090 Russia*
[c] *OOO Gazomotor-R, Rybinsk, Yaroslavl oblast, 152920 Russia*
**e-mail: vak@catalysis.ru*

Received February 20, 2013

Abstract—The problem of the thermochemical recuperation of heat from the exhaust gases of internal combustion engines (ICEs) as a method of increasing of the efficiency of fuels has been considered. The thermodynamic analysis of thermochemical recuperation conditions was performed, and maximum efficiency conditions were determined. Catalysts for the steam conversion of oxygen-containing fuels into syngas were developed, and the Co–Mn/Al_2O_3 catalyst was shown to be the most promising. The model of a thermochemical heat recuperation system was developed and manufactured, and its bench tests in the conversion of alcohols were performed using the simulated exhaust gases from a heating device. Mathematical models for calculating units of the heat recuperation system were developed. A recuperation system was manufactured and tested in the ICE-free and ICE-integrated variants. Based on the test results, the equivalent fuel consumption characteristics of a recuperative ICE was revealed to decrease by 11–22% depending on its load with a decrease in the concentration of hazardous emissions by 8–12 times for CO, 2–3.5 times for CH, and 18–25 times for NO_x.

DOI: 10.1134/S0040579513050187

INTRODUCTION

It is known [1] that the losses of heat energy entrained from spark-ignition ICEs into the environment with exhaust gases are 35%, the losses of heat withdrawn into the cooling circuit are 30%, heat losses due to the incomplete combustion of fuel are nearly 2%, and unaccounted heat losses are 3%. Theoretically, the losses of heat entrained into the environment and the cooling circuit can be recuperated, thereby increasing the heat efficiency. The essence of thermochemical recuperation (TCR) is that the heat withdrawn with exhaust gases and into the ICE cooling circuit is partially used for the endothermic conversion of an initial fuel into the other type of fuel with a higher enthalpy of products, thereby increasing the efficiency of fuel and ICE as a whole [2–12]. The conversion of fuels into syngas (mixture of CO and H_2) is the most energetically profitable solution. The scientific and methodological substantiation of this method of increasing the efficiency of ICEs was first given by Nosach [2], who called it thermochemical regeneration, and its practical implementation was applied to stationary solid-fuel systems.

There is a principal possibility of implementing two types of TCR, which can conditionally be called "external" and "internal." The external recuperation will be understood to mean the performance of the steam conversion of fuels only at the expense of engine exhaust gas heat (without recycling the exhaust gas itself). The scheme of external TCR is shown in Fig. 1.

In the case of external TCR, the selection of a fuel becomes principally important. As is known, the conversion of various fuels into a hydrogen-containing gas can be performed on catalysts. It is reasonable to use light homologues of saturated hydrocarbons, lower alcohols, and ethers as a potential source of syngas. The selection of fuel type for the generation of hydrogen is a compromise that takes into account the energy value of the fuel, the temperature conditions of conversion, the composition of a mixture after conversion, and the cost of syngas synthesis catalysts. In a series of works [3, 6, 7, 11], methanol and ethanol were selected to study TCR. An important feature that distinguishes these alcohols is a low temperature of their steam reforming and relatively cheap thermochemical conversion catalysts. The studies [3, 6, 7, 11] solve the problems of the technical implementation of external TCR aboard a transport vehicle. However, they do not absolutely consider the problems of the selection of catalysts, alcohol steam reforming conditions, a reactor type, and its operational regimes.

There is a rather high number of known studies on the development of catalysts for the steam reforming of

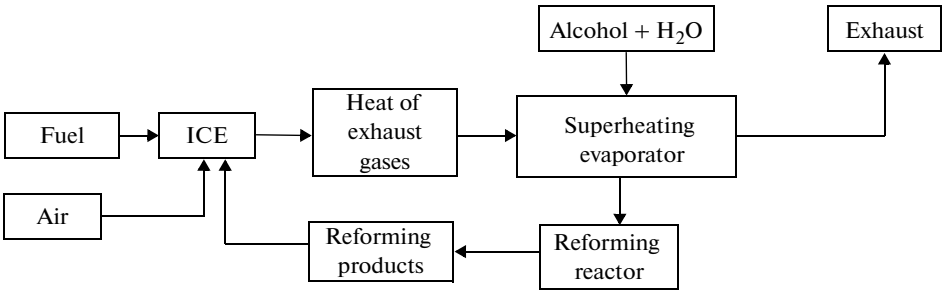

Fig. 1. Principal ICE flowsheet with external TCR.

methanol [13–19], ethanol [20–50], and ethers [51] with the purpose of the production of syngas. Copper-containing compounds, including metallic copper and its oxide, and different catalysts, which basic component is copper in combination with oxides of other metals, such as Cu–Zn, Cu–Mn, Cu–Al, Cu–Cr, etc., have been most widely and completely studied in the steam reforming of methane. At a temperature above 350°C, the copper-containing catalysts are gradually deactivated in the course of reaction due to the sintering of their active component. In connection with this, the $Cu/Al_2O_3–ZnO$, $Cu/Al_2O_3–Cr_2O_3$, and $Cu/Al_2O_3–MgO$ catalysts [16], the catalysts that represent Cu–Zr, Cu–Zr–Pd, and Cu–Z–Au amorphous alloys [17], and the platinoid-based catalysts [15, 16] were prepared and studied. Summarizing the literature results, we note that the methanol reforming reaction was studied at an H_2O/CH_3OH ratio varying in the range of 1–3, $V = 10000–30000\ h^{-1}$, a temperature of 300–700°C, and a pressure of 1–30 atm.

The steam ethanol reforming reaction was studied on cobalt supported [20–25], rhodium [23, 26–35], nickel [27, 36–46], nickel/copper [47–50], and palladium [29, 30, 34] catalysts. It was determined that these catalysts usually provide complete conversion in the steam reforming of ethanol at mixture hourly space velocities (GHSV) $V = 5000–100000\ h^{-1}$, temperatures of 500–700°C, and H_2O/C_2H_5OH ratios of 2–14. The catalysts based on rhodium and cobalt show the highest activity and stability in the steam reforming reaction, and the catalysts based on copper and nickel are the least active and stable [52].

As follows from the data on the steam reforming of alcohols on the copper- and nickel-containing catalysts the composition of reaction products corresponds to equilibrium values often. In the case of the rhodium- and cobalt-containing catalysts, the composition of reaction products is mostly nonequilibrium. Since, as will be shown in the theoretical part, this is the nonequilibrium reaction product composition that increases the efficiency of fuel, we used the rhodium and cobalt-containing catalysts as active components, when developing the catalysts for external TCR.

Internal TCR is more difficult to implement. Its essence consists of performing the endothermic catalytic CO_2/steam reforming of exhaust gases in a mixture with an initial motor fuel at the expense of heat that is entrained with exhaust gases and formed in the afterburning of oxygen contained in exhaust gases. This produces syngas in the composition of a mixed fuel, which is further used directly in the operational cycle of an engine. In the literature, this type of conversion has been called tri-reforming [53–58]. Since the typical composition of exhaust gases contains little oxygen ($CO_2 = 9–10\%$; $H_2O = 18–20\%$; $O_2 = 2–3\%$, nitrogen balance), the heat that is entrained with exhaust gases and generated in the oxidation of an initial fuel with residual oxygen may prove to be deficient for the endothermic CO_2/steam conversion of a fuel. In this case, the delivery of additional heat used in the cooling circuit of ICE is required. ICE with internal TCR is schematically exemplified in Fig. 2.

This scheme involves the partial recirculation of exhaust gases into a tri-reforming reactor with the addition of some fuel and heat from the engine cooling circuit to maintain heat balance.

Tri-reforming reactions proceed at higher temperatures and changed reagent ratios that considerably differ from the ratios for external recuperation using alcohols. The practical implementation of tri-reforming requires more complicated engineering solutions, and the selection of catalysts and the estimation of their service life and reaction conditions is one of the key problems [53–58].

The difficulty in developing tri-reforming catalysts consists of a great variety of simultaneous chemical reactions and the contrariety of their conditions. The available literature data that are partially summarized in Table 1 indicate the following catalyst activity order:

$$Ni/MgO > Ni/MgO/CeZrO_2 > NiCeO_2 \approx NiZrO_2 \approx NiAl_2O_3 > NiCeZrO_2.$$

Tri-reforming reactions (2)–(6) proceed at temperatures of 700–850°C, and the attainable conversion with respect to methane and CO_2 are at a level of 86–98 and 55–87%, respectively. The main problem emphasized by all researchers is that the propensity of nickel catalysts for coking restricts the duration of the performed experiments. To reduce coking, the catalysts doped with lanthanum, yttrium, copper, noble metals,

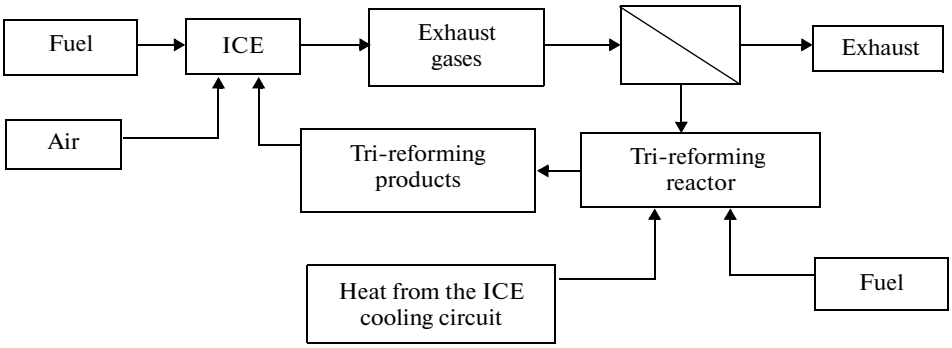

Fig. 2. Principal ICE flowsheet with internal TCRB.

chromium oxide, cerium, and zirconium are used. The modifications of nickel catalysts deposited onto alkali metal oxides like magnesium oxide have also proved to be promising [2, 4, 6].

The objective of our work is to perform the thermodynamic analysis of the efficiency of external TCR for the steam reforming of lower alcohols and the efficiency of internal TCR for the steam reforming of methane, to consider catalyst selection problems, to fulfill experimental studies on the external TCR model, the mathematical modeling of reactors for the catalytic reforming of methanol and ethanol and, finally, the experimental verification of the effect of external TCR on the improvement of the efficiency and environmental compatibility of ICE.

THEORY

Thermodynamic analysis of external TCR Conditions. In the given analysis, we shall consider four lower alcohols, such as methanol, ethanol, *n*-propanol, and *n*-butanol, which are intended to be used as syngas generation sources for external TCR. The thermodynamic data required for further analysis are listed in Table 2 [59].

Table 1. Catalysts and test conditions in tri-reforming reactions

No.	Catalysts	Test parameters and conditions	Source
1	Ni—La—CeO_2	$V = 30000\ h^{-1}$ $T = 800°C$ $t = 7.5$ h $CH_4/CO_2/O_2/H_2O = 1 : 0.46 : 0.1 : 0.46$	[53]
2	5.5%Ni/CeO_2; 3.8%Ni/ZrO_2; 6%Ni/Ce/ZrO_2; 8%Ni/MgO; 6.3%Ni/MgO/Ce/ZrO_2	$S_{sp} = 2.2–16.8\ m^2/g$ $T = 700–850°$ $CH_4/CO_2/O_2/H_2O = 1 : 0.475 : 0.1 : 0.475$ $CH_4/CO_2/O_2/H_2O = 1 : 1 : 0.1 : 1$ $CH_4/CO_2/O_2/H_2O = 1 : 0.375 : 0.5 : 0.375$	[54]
3	NiO/YSZ—CeO_2	$S_{sp} = 10.2\ m^2/g$ $V = 10000\ h^{-1}$ $T = 650–850°C$ $t = 120$ h $CH_4/CO_2/O_2/H_2O = 1 : 1 : 0.1 : 1$	[55]
4	Ni/MgO; Ni/$Mg_xTi_{1-x}O$	$S_{sp} = 28–46\ m^2/g$ $T = 850°C$ $t = 6$ h $CH_4/CO_2/O_2/H_2O = 1 : 0.48 : 0.1 : 0.54$	[57]
5	8%Ni/Al_2O_3	$S_{sp} = 367.5\ m^2/g$ $V = 2000–20000\ h^{-1}$ $T = 750–950°C$ $t = 10$ h $CH_4/CO_2/O_2/H_2O = 0.5 : 0.125 : 0.25 : 0.125$	[56]
6	NiO/MgO/CeO_2/ZrO_2/Al_2O_3	$T = 800°C$ $CH_4/CO_2/O_2/H_2O = 1 : 1.3 : 0.47 : 2.46$	[58]

Table 2. Some characteristics of considered alcohols [59]

Alcohol	Formula	T_b, °C	ΔH_{form} at $T = 25$°C, kJ/mol	ΔH_{vap} at $T = 25$°C, kJ/mol	ΔH_{vap} at $T = T_b$, kJ/mol	Q_{low} at $T = 25$°C, kJ/mol
Methanol	CH_3OH	65	201	37.5	35.3	677
Ethanol	C_2H_5OH	78	235	42	38.8	1279
n-Propanol	C_3H_7OH	97	257	48.3	41.8	1893
n-Butanol	C_4H_9OH	118	275	55.1	43.2	2511

Table 3. TCR efficiency μ under thermodynamic equilibrium in the steam reforming of alcohols. Calculation conditions: $T_{ref} = 500$°C, $P = 1$ bar, inlet H_2O/C ratio = 2

Alcohol	Dry mixture composition after steam reforming, mol %				Q_{comb}, kJ/mol	μ, %
	H_2	CO	CO_2	CH_4		
Methanol	55.7	3.0	22.7	18.6	660	3.2
Ethanol	51.9	3.3	22.5	22.3	1305	5.5
n-Propanol	50.3	3.4	22.5	23.8	1949	5.6
n-Butanol	49.7	3.5	22.4	24.4	2594	5.6

Let us select the ratio of the lower combustion heat of the thermochemical conversion products obtained from 1 mol of alcohol to a lower combustion heat of 1 mol of initial liquid alcohol as follows:

$$\mu = \left(\frac{Q_{comb}(\text{reforming products from 1 mol of alcohol})}{Q_{comb}(\text{1 mole of alcohol}) - \Delta H_{vap}(\text{1 mole of alcohol})} - 1 \right) \times 100\%, \quad (1)$$

as a TCR efficiency criterion for different alcohols and call it the TCR efficiency coefficient.

To estimate the increase in the efficiency due to thermochemical conversion, let us employ the data of thermodynamic calculations. The results of calculating the TCR efficiency by Eq. (1) for the thermodynamically equilibrium composition of a mixture in the steam reforming of alcohols are given in Table 3.

It follows from Table 3 that we should not expect a maximum increase in the TCR efficiency to exceed 6% the attainment of thermodynamic equilibrium in the steam conversion of lower alcohols. This is explained by the high outlet concentration of methane (18–24%) and therefore the weak endothermic effect of conversion under these conditions. An increase in the reforming temperature up to 700°C rises the coefficient μ to 16.4% for methanol and to 20.5% for ethanol. A change of the H_2O/C ratio from 2 to 11 increases the coefficient μ from 3.2 to 11% for methanol and from 5.5 to 14.6% for ethanol.

More optimistic results can be obtained when thermodynamic equilibrium is not attained. For example, this may occur when the conditions and catalysts are selected such that steam reforming yields only CO and H_2. This most energetically profitable TCR variant corresponds to the theoretically maximum endothermic effect of conversion and, consequently, the highest value of μ. The results of calculating the efficiency for this case are given in Table 4.

It follows from Table 4 that the value of μ in the case of TCR under nonequilibrium conditions for a number of lower alcohols (beginning from ethanol) varies slightly, and a possible increase in the TCR efficiency should be expected at a level of 20–25%.

Thermodynamic analysis of efficiency of internal TCR. Let us apply thermodynamic analysis to the use of natural gas as the main type of ICE fuel. In this case, the following possible chemical reactions of tri-reforming occur [53–58]:

$$CH_4 + CO_2 \leftrightarrow 2CO + 2H_2, \quad (2)$$

$$CH_4 + H_2O \leftrightarrow CO + 3H_2, \quad (3)$$

$$CO_2 + H_2 \leftrightarrow CO + H_2O, \quad (4)$$

$$CH_4 + 0.5O_2 = CO + 2H_2, \quad (5)$$

$$CH_4 + 2O_2 = CO_2 + 2H_2O. \quad (6)$$

Reactions (2)–(4) are endothermic, and reactions (5) and (6) are exothermic.

Let us determine the TCR efficiency coefficient for methane in a way similar to Eq. (1) for alcohols, but without the fuel vaporization term:

Table 4. Stoichiometrically maximum increase in TCR efficiency μ in reforming of alcohols into syngas under nonequilibrium conditions

Alcohol	Reaction	Q_{comb}, kJ/mol	μ, %
Methanol	$CH_3OH = CO + 2H_2$	768	20
Ethanol	$C_2H_5OH + H_2O = 2CO + 4H_2$	1535	24.1
n-Propanol	$C_3H_7OH + 2H_2O = 3CO + 6H_2$	2302	24.8
n-Butanol	$C_4H_9OH + 3H_2O = 4CO + 8H_2$	3070	25

$$\mu = \left(\frac{Q_{comb}(\text{reforming products from 1 mol of } CH_4)}{Q_{comb}(1\,\text{mole of } CH_4)} - 1 \right) \times 100\%, \quad (7)$$

where Q_{comb} is the lower combustion heat.

The internal TCR circuit (Fig. 2) with the partial recirculation of exhaust gases was calculated for natural gas, the delivery of only tri-reforming products into ICE (without mixing with additional natural gas), and the complete afterburning of combustible gases in ICE. The excess coefficient α of the air fed into the system (ICE + TCR circuit) was calculated with respect to the natural gas fed into ICE and varied within a range α = 1.1–1.4. The real air excess coefficient calculated with respect to the reforming products fed into ICE proved to be slightly higher than its calculated value due to additional air in the exhaust gas used for recirculation. The composition of the mixture leaving the tri-reforming reactor was determined from the condition of thermodynamic equilibrium at the outlet of the reactor at temperatures of 550–700°C. Taking into account the fact that the temperature of the exhaust gas withdrawn for recirculation may be much lower, namely, 350–600°C, and also the condition that the total heat effect of tri-reforming must be endothermic (otherwise, the TCR efficiency μ < 0), we intended to use the additional recuperation of heat withdrawn into the ICE cooling circuit to maintain the required temperature in the tri-reforming reactor.

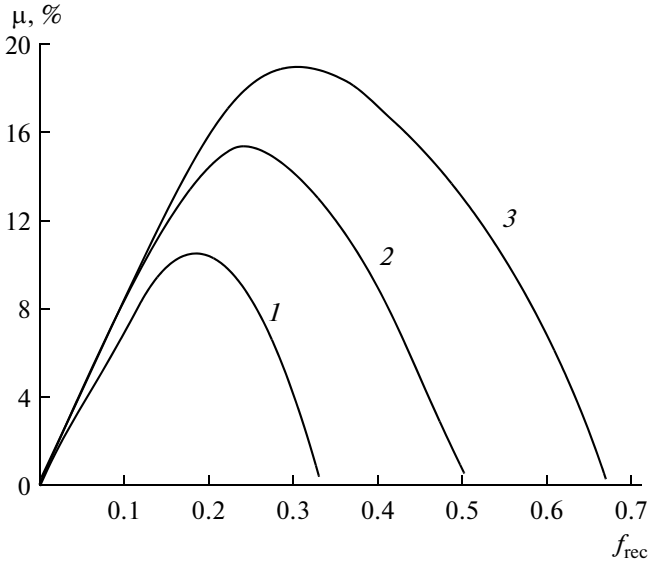

Fig. 3. TCR efficiency coefficient μ versus fraction of recirculated exhaust gases f_{rec} for the natural gas ICE at an air excess coefficient α of (*1*) 1.4, (*2*) 1.2, and (*3*) 1.1. Tri-reforming temperature, 700°C.

Since the composition of the ICE inlet mixture for the TCR scheme shown in Fig. 2 depends on the amount of initial fuel and the tri-reforming reactor's outlet product ratio governed by recirculation, the concentrations of components, and the fraction of ICE exhaust gases, as well as the stationary values of the material balance of this scheme, were found iteratively.

The results of calculating the TCR efficiency coefficient by Eq. (7) at an outlet tri-reforming reactor temperature of 700°C depending on the fraction of exhaust gases directed to recirculation f_{rec} and the excess coefficient α of air fed to ICE are shown in Fig. 3.

Similar results at a varied temperature and a constant air excess α = 1.1 are plotted in Fig. 4.

The plots can easily be observed to attain a maximum at changed f_{rec}. The existence of a maximum in these curves is explained by the fact that the exhaust gas contains oxygen, which additionally burns methane at a constant flow rate of natural gas at the inlet of the reforming reactor and an increasing exhaust gas recirculation, thus neutralizing the endothermic effect of tri-reforming. In other words, the presence of a maximum is due to the change in the ratio between endothermic and exothermic tri-reforming stages. In fact, the efficiency of internal recuperation is only increased due to endothermic reactions, and the growth of the flow rate of exhaust gases fed into the tri-reforming reactor actually leads to an increase in the flow rate of oxygen and the increasing contribution of exothermic reactions. This effect is confirmed by the calculation of the heat powers of the exothermic and endothermic stages at α = 1.1 and T_{ref} = 600°C and the total heat power of tri-reforming with a minimum at an optimal fraction f_{rec} = 0.38 (Fig. 5).

The mixture composition after the tri-reforming reactor for the given optimal point corresponds to the following composition (mol %): CH_4 = 2.47; CO_2 =

6.59; CO = 8.14; H_2 = 22.39; H_2O = 7.06; N_2 = 53.35. For comparison, let us give the composition of the mixture after the tri-reforming reactor for another optimal point (α = 1.4, T_{ref} = 700°C, f_{rec} = 0.17) as follows: 4.18 mol % CH_4, 1.15 mol % CO_2, 17.47 mol % CO, 35.71 mol % H_2, 1.51 mol % H_2O, and 39.98 mol % N_2.

Hence, there is an optimal fraction of exhaust gas withdrawn for the recirculation f_{rec} for the ICE scheme with internal TCR and exhaust gas recirculation. At $1.1 < \alpha < 1.4$ and $550 < T_{ref} < 700$°C, this optimal fraction is in the range of $0.17 < f_{rec} < 0.42$. Hence, it follows that the higher the air excess coefficient α and the reforming temperature, the smaller the fraction of exhaust gas that should be recycled.

EXPERIMENTAL

During experiments, we have performed studies on the development and testing of TCR catalysts and operational regimes for the TCR system model and, thus, the thermochemical heat recuperation block (TCRB) in the ICE-free and ICE-integrated variants.

Preparation and testing of external TCR catalysts. External TCR catalysts were developed using the technology described previously in [60]. The catalysts were prepared using porous nickel band as a support onto which aluminum oxide was deposited via impregnation from a saturated solution to form a substrate with subsequent drying and calcination. The active component was deposited onto thus prepared support via impregnation with a saturated aqueous solution containing nickel, cobalt, and rhodium compounds with subsequent drying and calcination at 450°C in a nitrogen flow. The catalysts were reduced in a hydrogen flow at 750°C, thus developing a specific surface area of the catalyst of up to 7–8 m^2/g. The $Co–Mn/Al_2O_3$, Rh/Al_2O_3, and Ni/Al_2O_3 catalysts for the steam reforming of methanol were prepared by this technology. Correspondingly, the $Co–Mn/Al_2O_3$, Rh/Al_2O_3, Ni/Al_2O_3, and Pt/Al_2O_3 catalysts were prepared for the steam reforming of ethanol. The catalysts were molded as monoliths with diameters of 16–18 mm and were installed inside a flow reactor during tests. The reactor represented an externally heated tube of 20 mm in diameter. Since the radial heat conductivity of a catalyst was at a level of 1–2 W/mK due to the metal porous support, no temperature gradients were observed along the radius. The composition of reaction products at the outlet of the reactor and the temperature of a catalyst at the inlet and outlet of the reactor were measured in experiments,. The catalyst load volume was 100 cm^3. The results of experiments on testing the catalysts are given in Tables 5 and 6.

It follows from Tables 5 and 6 that the conditions of thermodynamic equilibrium with respect to the composition of conversion products are attained on the nickel- and platinum-containing catalysts in the case of both methanol and ethanol. No equilibrium was observed on the $Co–Mn/Al_2O_3$ and Rh/Al_2O_3 for either methanol or ethanol, which agrees with the above literature data.

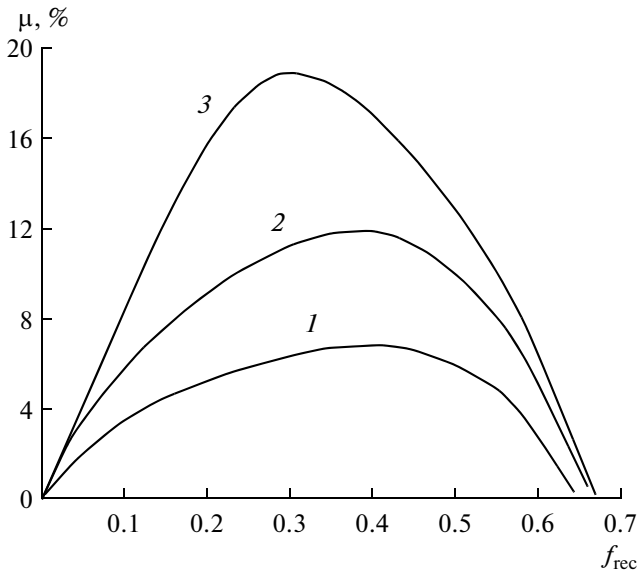

Fig. 4. TCR efficiency coefficient μ versus fraction of recirculated exhaust gases f_{rec} at an outlet tri-reforming reactor temperature of (*1*) 550, (*2*) 600, and (*3*) 700°C. Air excess coefficient for the natural gas ICE α = 1.1.

Developing TCRB model for external TCR. The objective of experiments on the TCRB model was to refine the data obtained previously in tests of the alcohol-reforming catalysts on the catalyst load, thermal regimes, and reagent conversions, and will be required

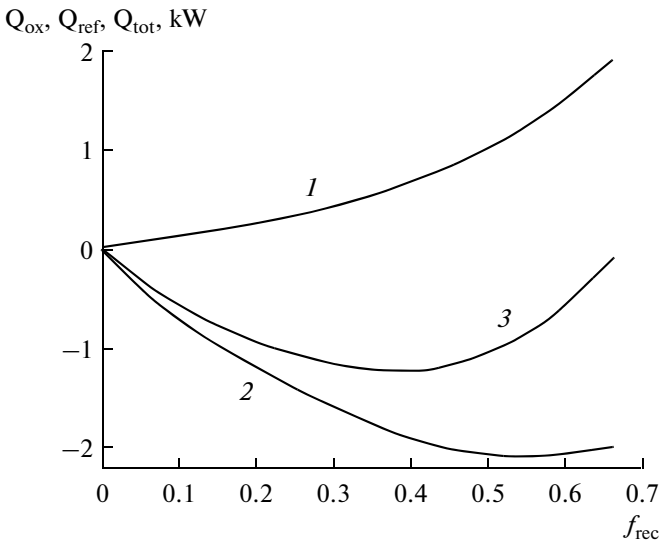

Fig. 5. Heat power of (*1*) exothermic stages Q_{ox} and (*2*) endothermic stages Q_{ref} and (*3*) total heat power Q_{tot} in tri-reforming versus fraction of recirculated exhaust gases f_{rec}. The calculation was performed at an inlet natural gas flow rate of the tri-reforming reactor of 1 m^3/h, α = 1.1, and a temperature of 600°C.

Table 5. Results of testing the $Co–Mn/Al_2O_3$ catalyst in the reforming of methanol (molar ratio $H_2O/CH_3OH = 1.3 : 1$)

No.	Flow rate ($H_2O + CH_3OH$), g/h	T_{ref}, °C	Composition of dry reforming products, vol %			
			H_2	CO	CO_2	CH_4
1	159	506	68.5	9.3	20.4	0.96
2	159	480	67.5	13.1	16.5	0.62
3	170	479	67.4	13.2	16.3	0.66
Thermodynamic equilibrium		479	46.2	2.5	23.1	28.2

Table 6. Results of testing the $Co–Mn/Al_2O_3$ catalyst in the reforming of ethanol (molar ratio $H_2O/C_2H_5OH = 4 : 1$)

No.	Flow rate ($H_2O + C_2H_5OH$), g/h	T_{ref}, °C	Composition of dry reforming products, vol %			
			H_2	CO	CO_2	CH_4
1	46	517	59.1	5.3	23.2	13.4
2	70	516	51.4	1.1	18	6.8
3	50	516	50.69	1.2	18.7	6.1
Thermodynamic equilibrium		516	54.7	4.2	21.9	18.9

to develop the TCRB and its experimental studies in combination with ICE.

The TCRB model consisted of a heating device, steam alcohol reformer, and a network of capillaries for the delivery of liquids. The construction of the reformer for the generation of syngas from aqueous oxygen-containing fuel (methanol, ethanol) solutions represented a device that consisted of an inner 20-mm-diameter tube filled with a catalyst and placed inside an external tube with a diameter of 40 mm and a length of 450 mm. The catalyst had good thermal contact with the metal wall and modeled the structural elements of catalytic panels due to its high heat conductivity and metal porous structure. A hot gas that simulates the exhaust gases of an engine was supplied countercurrently with respect to the reaction mixture from the heating device into the space between the external and internal tubes. A water–alcohol mixture evaporator consisting of thin-wall tubes that were blown over by hot air obtained in the heating device was installed in the same place. The saturated vapor from the evaporator entered a vapor superheater to be delivered to the reforming reactor. A heating device presented the burner described in detail in the patent [61] was used as a source model of the exhaust gases of an engine. The temperature of the hot gas from the heating device was adjusted by two-stage air supply. Air 1 was supplied at the first stage for the combustion of fuel and air 2 was supplied at the second stage to dilute the oxidation products and to attain a required temperature. These data are given in Table 7.

The TCRB model was installed on a bench to perform its testing and develop the regimes of the conversion of a hydrocarbon feedstock into syngas. The bench consisted of a vessel for the storage of reagents; a supply and flow rate control system; a temperature display and recording system; a superheating evaporator for a water–alcohol mixture; the TCRB model; and a Siemens gas analyzer that provided the continuous measurement of the CH_4, CO, CO_2, and H_2 concentrations. The start-up of the system was begun with the supply of hot alcohol oxidation products obtained in the heating device in the intertube space of the reactor. After the catalyst bed temperature attained 500°C, the water–alcohol mixture was fed into the evaporator, where it was vaporized. Then, the vapor mixture was delivered to the vapor superheater and, after heating to no less than 370°C, it was delivered to the inlet of the TCRB model. A heat transfer agent that supplied heat required for the endothermic steam alcohol reforming reaction to the catalyst bed was fed into the intertube space. After the steady-state regime was attained, the reforming products were sampled at the outlet of the TCRB model and analyzed in the continuous regime on a Siemens gas analyzer. The results of experiments are given in Table 7.

It follows from the experimental data given in Table 7 that the near-complete conversion of methanol is achieved at outlet temperatures of the steam methanol reforming reactor of 266–390°C, temperatures of the gases simulating ICE exhaust gases of 373–520°C, and GHSV $V = 10000–15000$ h^{-1}. The concentration of hydrogen in the reaction products is nearly 70 vol %. The experimental data obtained on the TCRB model were used as initial data to develop the TCRB and test it experimentally in combination with ICE.

Development of TCRB for external TCR. To analyze the experimental data and the possibility of using the obtained results to develop TCRB operated in combination with ICE in the regime of external TCR, we used the two-dimensional mathematical model of a conversion reactor integrated with an evaporator and vapor superheater of in the variants of panel and tube types. In the model, the heat balance equations took into account the axial convective heat transfer by gas, the radial (transversal) heat transfer over the catalysts bed, and the heat transfer between the reaction gas and the catalyst. The mathematical model of the processes in exothermic channels represented a one-dimensional plug-flow model. The model took into account the convective heat transfer by the heating gas and the heat exchange between this gas and the wall of a panel or a tube. In the material balance equations for endothermic channels, we used the three-stage scheme of the reactions of (1) steam alcohol reforming, (2) steam CO reforming, and (3) alcohol decomposition.

The kinetic parameters of the models were estimated from the data [62] for ethanol and [63] for methanol with the refinement of kinetic constants in compliance with the experimental data obtained in this work. The

Table 7. Results of testing TCRB model in steam reforming of methanol

No.	Flow rates into the heating device, L/min			Flow rates to reforming, g/h		T, °C		Composition of dry reforming products, vol %			
	CH_4	air 1	air 2	CH_3OH	H_2O	inlet hot gases	TCRB outlet gases	CO	CO_2	CH_4	H_2
1	9	90	260	640	360	520	383	7.8	22	0.068	69.4
2	9	90	300	640	360	462	390	8.3	21.2	0.041	69.7
3	9	90	300	640	360	457	384	6.8	22.6	0.025	70.0
4	9	90	300	800	450	450	375	6.7	22.6	0.086	70.0
5	9	90	360	800	450	427	360	6.3	23.1	0	70.1
6	9	90	360	800	450	425	338	5.5	24	0	70.2
7	9	90	370	800	450	418	332	5.3	24.1	0	70.2
8	9	90	400	800	450	407	325	4.7	24.5	0	70.3
9	9	90	420	800	450	391	318	4.8	24.6	0	70.2
10	9	90	420	800	450	389	308	4.3	25.2	0	70.3
11	9	90	420	1200	675	373	271	3.1	26.2	0	70.5
12	9	90	420	1200	675	373	266	2.7	26.7	0	70.5

parameters of mass and heat transfer processes were calculated by the correlations [64].

The results calculated by the mathematical model with the experimental data obtained on the TCRB model in the case of methanol are compared in Fig. 6–8. It follows from the given comparison that the mathematical model describes the experimental data obtained on the TCRB model rather well and can be used to calculate the dimensions and operational regimes of the heat recuperation unit.

The problem of the numerical analysis of TCRB included calculating the distributions of concentrations and temperatures for different process variants (concurrent and countercurrent) and reactor dimensions. At a specified flow rate of hot exhaust gases from the engine (46–58 kg/h), we calculated the dimension of different units of the system provided an alcohol conversion of no less than 98% at an alcohol flow rate of 5–6 kg/h and a water flow rate of nearly 3 kg/h. The calculations were performed for the panel and tube reactors for methanol and ethanol, respectively.

Based on the results of calculating the methanol reformer, we selected the panel reactor detailed in [65]. The reactor consists of catalytic endothermic panels and flat exothermic channels with the following parameters:

(1) the catalytic panels have a thickness of 18 mm, a width of 180 mm, and a length of 400 mm; the number of panels is 9 and the catalyst volume is 12 L;

(2) the exothermic panels have a thickness of 4 mm, a width of 180 mm, and a length of 400 mm, and the number of panels is 10;

(3) the reagent and heating gas flows in corresponding panels are concurrent.

The photos of the TCRB assembly and the structure of alternating catalytic endothermic and exothermic panels are shown in Fig. 9.

In the case of ethanol, the reactor consists of a tube apparatus, the tubes of which are filled with a catalyst and blown over by hot gases from heating device or the exhaust gases from ICE. The results of calculating the distributions of temperatures and conversion along the catalyst bed length for the countercurrent and concurrent flows of the reagents and the heating gas are plotted in Fig. 10.

Based on the performed calculations we have determined the following process parameters of the reactor and the heat exchanger integrated with it in the range of

ICE exhaust gas temperatures of 500–620°C, at flow rates of 46–58 kg/h, for the total heat power of 30 kW:

(1) the calculated specific capacity of the reactor is 3–5 m^3 gas/(h L) or 2–3 m^3 $(CO + H_2)$/(h L) at ethanol and water flow rates of 3.9 and 6.14 kg/h;

(2) tubes filled with a catalyst are 20 mm in diameter and 700 mm in length, and their number is 25;

(3) under these conditions, the external TCR efficiency coefficient μ lies within 12–16%.

Under the considered conditions, the reactors with both countercurrent and concurrent exhaust and conversion gas flows provide 100% conversion at the outlet (Fig. 10c). However, the predominant fraction of ethanol is converted in the hot zone near the heating gas injection. The opposite zone of the reactor has very low temperature and conversion (Fig. 10a). The alternative concurrent scheme provides a more uniform temperature profile along the length (Fig. 10b) and, consequently, an ethanol conversion that is more stable under

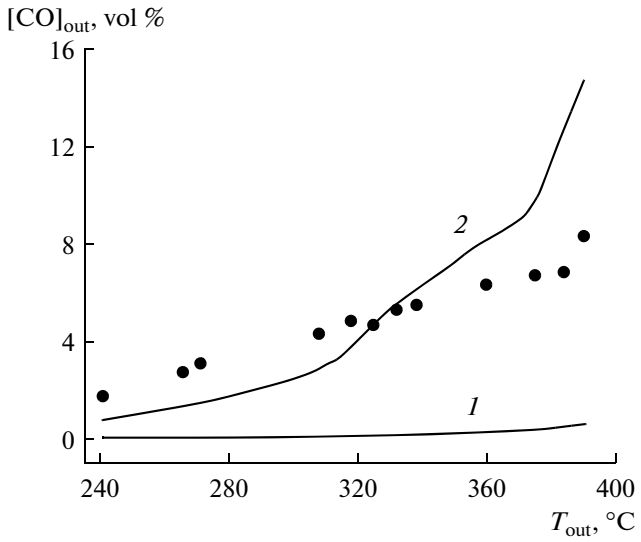

Fig. 6. Comparison of experimental CO dry-gas concentrations (points) with (*1*) thermodynamic equilibrium and (*2*) calculation by mathematical model depending on outlet TCRB model temperature.

heat losses (Fig. 10c) and is preferable from the practical viewpoint.

The results of short-time tests of the two reactor types without ICE and using a heating device to simulate hot exhaust gases are given in Tables 8 and 9. These results show that the TCRB capacity is acceptable for further studies in experiments with ICE.

Experimental studies of TCRB system integrated with ICE. The experimental studied of the TCRB integrated with ICE were performed on the bench, the main units of which were a thermochemical conversion unit, a microprocessor-based control system (MCS), ICE of the ZMZ-40522 type, gas analysis equipment, a system for taking syngas samples from TCRB, and from the mixture of outlet exhaust gases. The gas analysis equipment consisted of an AVP-02G hydrogen analyzer (TU (Technical Specifications) 4215-002-16963232-03), a MEXA-441GE exhaust gas emission analyzer, and an AGM-505.1 DKIN.413411.001TU NO_x gas analyzer. MCS represented a separate unit, controlled the operational regimes of the bench, and entered the information into a computer for further analysis. The bench was also equipped with systems for studying the operational characteristics of an engine in different operational regimes, including an operation in combination with the TCR unit. The experimental studies were performed using gasoline as the main fuel and methanol and ethanol for the thermochemical recuperation of heat.

The objectives of the performed studies were as follows:

(1) to determine the regions and regimes of the stable operation of TCRB in combination with ICE;

(2) to study the effect of the additions of syngas from the external TCR of methanol and ethanol to the main fuel on the fuel efficiency of ICE;

(3) to study the effect of the additions of syngas from the external TCR on the emission of ICE exhaust gases.

After the adjustment and startup procedures on the bench, the ICE load characteristics were experimentally checked to select an optimal ICE operation regime with respect to the temperature of exhaust gases and to provide the ICE motor power required for the study of

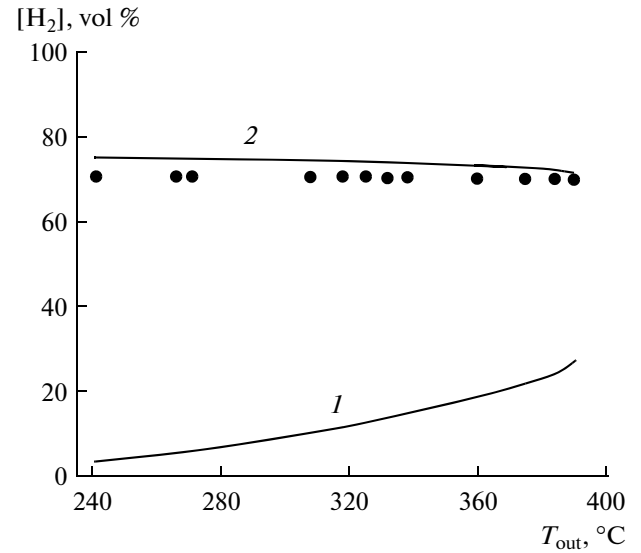

Fig. 7. Comparison of experimental H_2 dry-gas concentrations (points) with (*1*) thermodynamic equilibrium and (*2*) calculations by mathematical model depending on outlet TCRB model temperature.

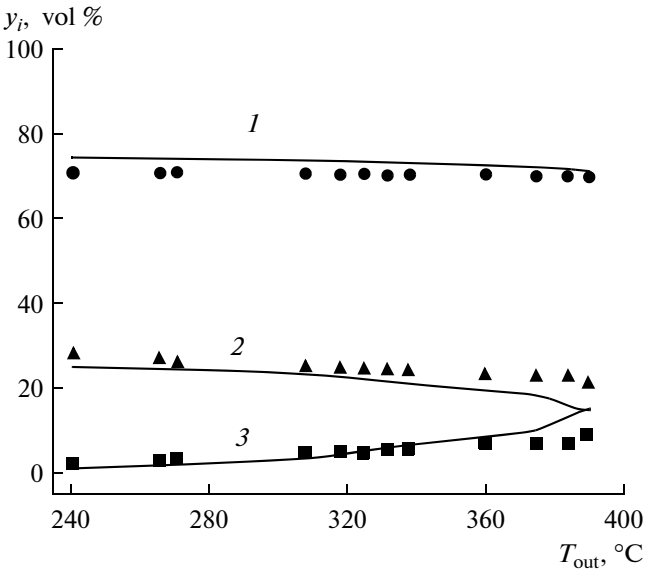

Fig. 8. Comparison of experimental dry-gas concentrations y_i of H_2 (rounds), CO_2 (triangles), and CO (squares) with calculations by mathematical model for (*1*) H_2, (*2*) CO_2, and (*3*) CO depending on outlet TCRB model temperature.

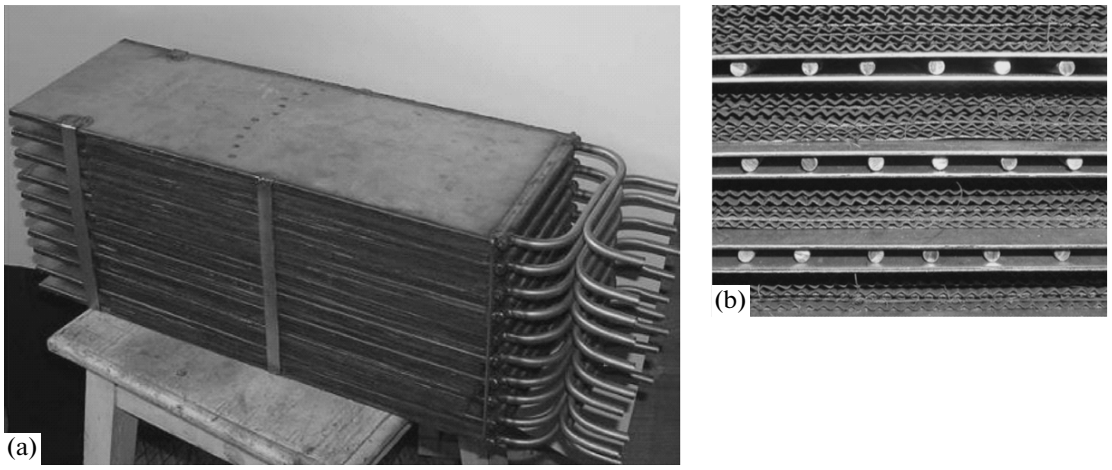

Fig. 9. General view of (a) TCRB assembly and (b) structure of exothermic and endothermic panels.

Table 8. Tests of TCRB in thermochemical conversion of methanol

No.	Flow rates to conversion, kg/h		T_{conv}, °C	[CO + H_2], dry vol %	Composition of dry conversion products, vol %			
	CH_3OH	H_2O			H_2	CO	CO_2	CH_4
1	5.1	3.73	517	77.8	62.1	15.7	13.8	8.4
2	5.1	5.74	510	77.5	70.8	6.7	22.1	0.4

Table 9. Tests of TCRB in thermochemical conversion of ethanol

No.	Flow rates to conversion, kg/h		T_{conv}, °C	[CO + H_2], dry vol %	Composition of dry conversion products, vol %			
	C_2H_5OH	H_2O			H_2	CO	CO_2	CH_4
1	3.9	4	518	79.90	69.9	10	20	3.1
2	3.9	6.14	510	64.6	60.5	4.2	21.8	13.5

Table 10. Effect of TCRB on efficiency and environmental compatibility of ICE

Experimental conditions					
$\alpha = 1$, $G_{syn} = 0$					
N_e, kW	8.4	17.1	22.5	25.7	30.5
[CO], %	0.72	0.87	0.95	1.12	1.37
[CO], ppm	112	125	198	275	370
[CO_x], ppm	1100	1280	1720	2100	2550
G_{gasol}, kg/h	3.71	4.1	4.79	5.8	6.93
$\alpha = 1.8$, $G_{syn} = 15.8$ m^3/h					
[CO], %	0.06	0.08	0.11	0.13	0.18
[CO], ppm	54	63	72	89	105
[CO_x], ppm	47	54	76	110	142
G_{eqv}*, kg/h	2.95	3.41	4.10	5.15	6.23

* Hereinafter, equivalent fuel is understood to mean fuel that consists of main fuel and syngas obtained via the thermochemical recuperation of ICE exhaust gas heat and provides the combustion heat sufficient to maintain ICE operational regimes.

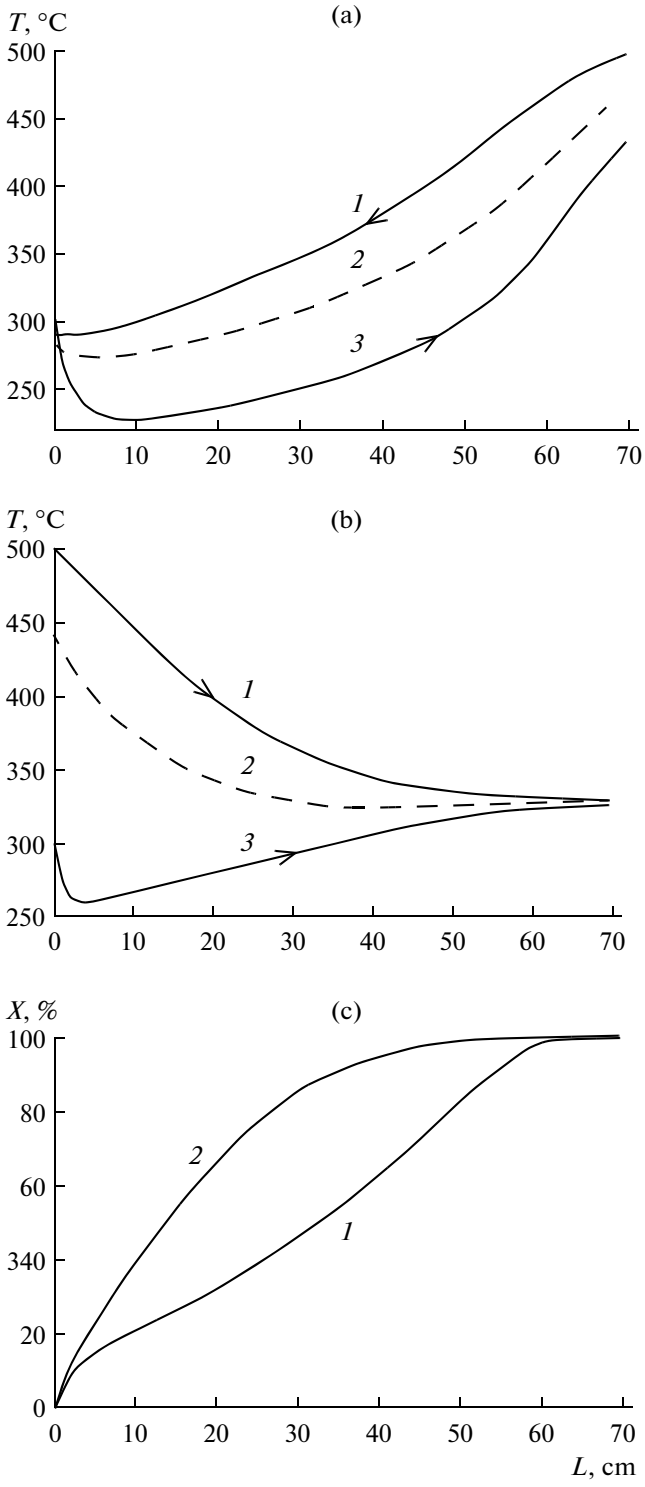

Fig. 10. Results of calculating temperature distribution for (a) countercurrent and (b) concurrent: (*1*) exhaust gas, (*2*) tube wall, (*3*) catalyst; (c) comparison of the ethanol conversion profile for (*1*) countercurrent and (*2*) concurrent. The ICE exhaust gas temperature at inlet of convertor is 500°C. Ethanol flow rate is 3.9 kg/h; water flow rate is 6.14 kg/h; $H_2O/C = 2$.

regimes with consideration for the fuel flow rate, the dynamic characteristics, and the service life. As follows from the performed experiments on the load characteristics, the most suitable regime for the operation with ICE is the regime, in which the temperature of exhaust gases does not decrease below 370°C throughout the entire range of loads, and the motor power is equal to 30 kW, i.e., 60% of the load characteristic and provides a required power allowance of no less than 12–15% in the case of abrupt ICE load changes. Top estimate the quantitative characteristics on the possible decrease in the fuel flow rate due to mechanical (pumping) losses, we measured the actual pumping losses of the ZMZ-40522.10 type ICE for different positions of its throttle. As a result of these experiments, it has been shown that the pumping losses are 10–11% on the average in the operation of IVE on the main fuel and stoichiometric mixtures at a number of revolutions n = 3000 rpm. Hence, the pumping losses and the equivalent fuel flow rate should be expected to decrease by no less than 5% upon the passage to the operation of ICE on lean mixtures with the additions of syngas to the main fuel.

The summarized experimental data on the effect of the additions of syngas obtained as a result of thermochemical heat recuperation in TCRB to the main fuel fed into ICE for the steady state regime at a number of crankshaft revolutions n = 3000 rpm are given in Table 10. The upper part of Table 10 contains the experimental data for the operation of ICE on the main fuel and a stoichiometric fuel–air mixture (air excess coefficient $\alpha = 1$) without syngas additions. The lower part of Table 10 contains the data for the supply of syngas obtained as a result of external TCR in a mixture with air into the ICE air receiver at $\alpha = 1.8$. The syngas was obtained in TCRB in the conversion of alcohols (methanol and ethanol) using the heat of the ICE exhaust gases. It can be seen from Table 10 that the operation of ICE with TCRB not only considerably improves the consumption characteristics of an engine with respect to equivalent fuel from 11 to 22% depending on the load, but also decreases the concentrations of hazardous emissions by 8–12 times for CO, 2–3.5 times for CH, and by 18–25 times for NO_x.

CONCLUSIONS

The results obtained in the present work clearly demonstrate the prospects of using the thermochemical recuperation of ICE exhaust gases for improving the fuel efficiency. The efficiency acquired with respect to fuel consumption considerably exceeds the data [12], which show an 8.5% decrease in the consumption of fuel at a slight decrease in the emission. The results of our work on improving efficiency slightly exceed the results of the work [2], where this value was estimated for ICE to be 10–15%, and agree well with the theoretical estimates [8]. It is possible to distinguish the following reasons for the decrease in the fuel flow rate in the

case of thermochemical recuperation. First, this is a minimum 6% decrease in the mechanical (pumping) losses upon the passage of ICE to lean mixtures (α = 1.8) due to the addition of hydrogen-containing gas. These data agree with the results obtained earlier in the study of the effect of syngas additions on the operation of ICE with the using natural gas as a fuel [66]. The second reason for the decrease in the fuel flow rate is associated with the thermochemical recuperation of ICE exhaust gases via the conversion of alcohol into syngas. This provides an equivalent fuel conservation of no less than 13–14%. Moreover, the additions of a hydrogen-containing gas to the main fuel decreases the size of the exclusion zone in the ICE combustion chamber (the zone near the walls of the ICE cylinder and head), thus increasing the completeness of the combustion of equivalent fuel even in the case of lean mixtures, which also decreases the consumption of fuel. Similar results were obtained for the additions of syngas to the binary fuel fed into a diesel engine [67]. So the total saving of equivalent fuel changes from 22 to 11% with increasing load.

Hence, the use of thermochemical heat recuperation is a real low-cost method of increasing the efficiency of fuels in ICEs and opens the possibilities of the creation of new efficient variants for the application of catalytic technologies in ICEs.

ACKNOWLEDGMENTS

This work was supported by the Development Foundation of the Center for Development and Commercialization of New Technologies (Skolkovo Innovation Center), grant agreement no. 64 (UNIHEAT project).

NOTATION

f_{rec}—fraction of recirculated ICE exhaust gases;
G_{gas}—gasoline flow rate, kg/h;
G_{syn}—syngas flow rate, m^3/h;
G_{eqv}—equivalent fuel flow rate, kg/h;
ΔH_{vap}—specific vaporization heat, kJ/mol;
ΔH_{form}—specific heat of formation in the gas phase, kJ/mol;
N_e—effective ICE power, kW;
n—number of revolutions, rpm;
P—pressure, bar;
Q_{comb}—lower combustion heat of the reformate produced from of 1 mole of alcohol; kJ/mol;
Q_{low}—lower heating value of alcohols in gas phase, kJ / mol;
Q_{ox}—heat power of exothermic stages, kW;
S_{sp}—specific surface area of a catalyst, m^2/g;
T_{ref}—steam reforming or tri-reforming temperature, °C;
T_b—normal boiling temperature, °C;
T_{conv}—conversion temperature, °C;
t—time of tests, h;
V—mixture hourly space velocity, h^{-1};
X—conversion, %;
α—air excess coefficient;
μ—TCR efficiency coefficient, %.

REFERENCES

1. *Dvigateli vnutrennego sgoraniya: Teoriya porshnevykh i kombinirovannykh dvigatelei* (Internal Combustion Engines: Theory of Reciprocating and Combined-Cycle Engines), Orlin, A.S. and Kruglov, M.G., Eds., Moscow: Mashinostroenie, 1983.
2. Nosach, V.G., Methods of increasing the fuel use efficiency in technological processes, *Teplofiz. Teplotekh.*, 1967, no. 7, p. 44.
3. Ipatov, A.A., Kamenev, V.F., Khripach, N.A., and Lezhnev, L.Yu., Development and study of vehicles with different types of hydrogen and combined engines, *Zh. Avtomob. Inzh.*, 2007, no. 5, p. 18.
4. Hoseman, G. and Cerini, W.G., On-board generator supplies H_2 for I-C engine, *Autom. Eng.*, 1974, vol. 82, no. 8, p. 42.
5. Shrainer, D.D., USSR Inventor's Certificate no. 1275100, *Byull. Izobret.*, 1986, no. 45.
6. Zvonov, V.A., Chernykh, V.I., and Balakin, V.K., *Metanol kak toplivo dlya transportnykh dvigatelei* (Methanol as a Fuel for Automotive Engines), Kharkov: Osnova, 1990.
7. Zvonov, V.A., Krupnik, L.I., Chernykh, V.I., et al., USSR Inventor's Certificate no. 1184965, *Byull. Izobret.,* 1985, no. 38.
8. Khripach, N.A., Improvement of Environmental and Fuel-Saving Characteristics of a Forced-Ignition Engine by Preliminary Thermochemical Reforming of Methanol, *Cand. Sci. (Eng.) Dissertation*, Moscow: Moscow State Univ. of Mechanical Engineering, 2004.
9. Fomin, V.M., Kamenev, V.F., and Khripach, N.A., Improvement of the duty cycle of a forced-ignition internal combustion engine and thermochemical recovery of withdrawn heat, *Obrazovanie cherez nauku: Sbornik trudov mezhd. simp.* ("Education through Science," Proc. Int. Symp.), Moscow, 2005, p. 142.
10. Ouchi, T., Japanese Patent 61141927, 1986.
11. Amphlett, J.C., Evans, M.J., Jones, et al., Hydrogen production by the catalytic steam reforming of methanol, *Can. J. Chem. Eng.*, 1981, vol. 59, p. 720.
12. Allen, J., Soinski, A., and Koyama, K., *Thermochemical Fuel Reforming for Reciprocating Internal Combustion Engines*, PIER Final Project Report of Gas Technol. Inst. CEC-500—2009-011, 2011, p. 35.
13. Takezawa, N. and Iwasa, N., Steam reforming and dehydrogenation of methanol: difference in the catalytic functions of copper and group VIII metals, *Catal. Today*, 1997, vol. 36, p. 45.
14. Suwa, Y., Ito, S., Kameoka, et al., Comparative study between Zn–Pd/C and Pd/ZnO catalysts for steam reforming of methanol, *Appl. Catal., A*, 2004, vol. 267, p. 9.
15. Suwa, Y., Ito, S., Kameoka, S., et al., Steam reforming of methanol over Pt–Zn alloy catalyst supported on carbon black, *Catal. Commun.*, 2003, vol. 4, p. 499.

16. Sekizawa, K., Utaka, T., and Eguchi, K., Catalytic production of hydrogen from methanol for fuel cell application, *Kinet. Catal*, 1999, vol. 40, p. 411.
17. Takahashi, T., Inoue, M., and Kai, T., Effect of metal composition on hydrogen selectivity in steam reforming of methanol over catalysts prepared from amorphous alloys, *Appl. Catal., A*, 2001, vol. 218, p. 189.
18. Matsumura, Y. and Shen, W., Methanol decomposition and synthesis over palladium catalysts, *Top. Catal.,* 2003, vol. 22, p. 271.
19. Shishido, T., Sameshima, H., and Takehira, K., Methanol decomposition to synthesis gas over supported Pd catalysts prepared from hydrotalcite precursors, *Top. Catal.*, 2003, vol. 22, p. 261.
20. Liguras, D.K., Kondarides, D.I., and Verykios, X.E., Production of hydrogen for fuel cell by steam reforming of ethanol over supported noble metal catalysts, *Appl. Catal., A*, 2003, vol. 43, p. 345.
21. Diagne, C., Idriss, H., and Kiennemann, A., Hydrogen production by ethanol reforming over $Rh/CeO_2–ZrO_2$, *Catal. Commun.*, 2002, vol. 3, p. 565.
22. Wanat, E.S., Venkataraman, K., and Shmidt, L.D., Steam reforming and water–gas shift of ethanol on Rh and Rh–Ce catalysts in a catalytic wall reactor, *Appl. Catal., A,* 2004, vol. 276, p. 155.
23. Aupretre, F., Descorme, C., Duprez, D., et al., Ethanol steam reforming over $Mg_xNi_{1-x}Al_2O_3$ spinel oxide–supported Rh catalysts, *J. Catal.,* 2005, vol. 233, p. 464.
24. Frusteri, F., Freni, S., Spadaro, L., et al., H_2 production for MC fuel cell by steam reforming of ethanol over MgO supported Pd, Rh, Ni and Co catalysts, *Catal. Commun.*, 2004, vol. 5, p. 611.
25. Raskó, J., Hancz, A., and Erdohelyi, A., Surface species and gas phase products in steam reforming of ethanol on TiO_2 and Rh/TiP_2, *Appl. Catal., A*, 2004, vol. 269, p. 13.
26. Fatsikostas, A., Kondarides, D., and Verykios, X., Steam reforming of biomass-derived ethanol for the production of hydrogen for fuel cell applications, *Chem. Commun.*, 2001, vol. 9, p. 851.
27. Lee, S., Ahmed, S., and Ahluwalia, R., Steam reforming of ethanol at elevated pressure for hydrogen production, *Proc. 2006 Fuel Cell Seminar*, Hawaii, 2006, Rep. 000401.
28. Fatsikostas, A.N., Kondarides, D.I., and Verykios, X.E., Production of hydrogen for fuel cells by reformation of biomass-derived ethanol, *Catal. Today*, 2002, vol. 75, p. 145.
29. Llorca, J., de la Piscina, P.R., Dalmon, J-A., Sales, J., and Homs, N., Co-free hydrogen from steam-reforming of bioethanol over ZnO-supported cobalt catalysts. Effect of the metallic precursor, *Appl. Catal., B*, 2003, vol. 43, p. 355.
30. Batista, M.S., Santos, R.K.S., Assaf, E.M., et al., High efficiency steam reforming of ethanol by cobalt-based catalysts, *J. Power Sources*, 2004, vol. 134, p. 27.
31. Llorca, J., Homs, N., Sales, J., er al., Effect of sodium addition on the performance of Co–ZnO-based catalysts for hydrogen production from bioethanol, *J. Catal.*, 2004, vol. 222, p. 470.
32. Cavallaro, S., Mondello, N., and Freni, S., Hydrogen produced from ethanol for internal reforming molten carbonate fuel cell, *J. Power Sources*, 2001, vol. 102, p. 198.
33. Kaddouri, A. and Mazzocchia, C., A study of the influence of the synthesis conditions upon the catalytic properties of Co/SiO_2 or Co/Al_2O_3 catalysts used for ethanol steam reforming, *Catal. Commun.*, 2004, vol. 5, p. 339.
34. Batista, M.S., Santos, R.K.S., Assaf, E.M., et al., Characterization of the activity and stability of supported cobalt catalysts for the steam reforming of ethanol, *J. Power Sources*, 2003, vol. 124, p. 99.
35. Freni, S., Rh based catalyst for indirect internal reforming ethanol application in molten carbonate fuel cells, *J. Power Sources*, 2001, vol. 94, p. 14.
36. Aupretre, F., Descorme, C., and Duprez, D., Bio-ethanol catalytic steam reforming over supported metal catalysts, *Catal. Commun.,* 2002, vol. 3, p. 263.
37. Cavallaro, S., Chiodo, V., Freni, et al., Performance of Rh/Al_2O_3 catalyst in the steam reforming of ethanol: H_2 production for MCFC, *Appl. Catal., A*, 2003, vol. 249, p. 119.
38. Breen, J.P., Burch, R., and Coleman, H.M., Metal-catalyzed steam reforming of ethanol in the production of hydrogen for fuel cell application, *Appl. Catal. B,* 2002, vol. 39, p. 65.
39. Jie, Sun., Xinping, Qiu., Feng, Wu., et al., Steam reforming of ethanol in low and middle temperature range for fuel cell application, *Int. J. Hydrogen Energy*, 2004, vol. 29, p. 1075.
40. Jie, Sun., Xin-Ping, Qui., Feng, Wu., et al., H_2 from steam reforming of ethanol at low temperature over Ni/Y_2O_3, Ni/La_2O_3 and Ni/Al_2O_3 catalysts for fuel-cell application, *Int. J. Hydrogen Energy*, 2005, vol. 30, p. 437.
41. Fatsikostas, A.N. and Verykios, X.E., Reaction network of steam reforming of ethanol over Ni-based catalysts, *J. Catal.*, 2004, vol. 225, p. 439.
42. Frusteri, F., Freni, S., Chiodo, V., et al., Potassium improved stability of Ni/MgO in the steam reforming of ethanol for the production of hydrogen for MCFC, *J. Power Sources*, 2004, vol. 132, p. 139.
43. Comas, J., Marino, F., Laborde, M., and Amadeo, N., Bioethanol steam reforming on Ni/Al_2O_3, *Chem. Eng. J.,* 2004, vol. 98, p. 61.
44. Frusteri, F., Freni, S., Chiodo, V., et al., Steam reforming of bio-ethanol on alkali-doped Ni/MgO catalyst: hydrogen production for MC fuel cell, *Appl. Catal., A*, 2004, vol. 270, p. 1.
45. Srinivas, D., Satyanarayana, C.V.V., Potdar, H.S., and Ratnasamy, P., Structural studies on $Ni–CeO_2–ZrO_2$ catalyst for steam reforming of ethanol, *Appl. Catal., A*, 2003, vol. 246, p. 323.
46. Freni, S., Cavallaro, S., Mondello, N., et al., Production of hydrogen for MC fuel cell by steam reforming of ethanol over MgO supported Ni and Co catalyst, *Catal. Commun.*, 2003, vol. 4, p. 259.
47. Marino, F., Boveri, M., Baronetti, G., and Laborde, M., Hydrogen production from steam reforming of bioethanol using $Cu/Ni/K/\gamma\text{-}Al_2O_3$ catalysts: effect of Ni, *Int. J. Hydrogen Energy*, 2001, vol. 26, p. 665.
48. Marino, F., Baronetti, G., Jobbagy, M., and Laborde, M., $Cu–Ni–K/\gamma\text{-}Al_2O_3$ supported catalysts for ethanol steam reforming: formation of hydrotalcite-type com-

pounds as a result of metal–support interaction, *Appl. Catal., A,* 2003, vol. 238, p. 41.

49. Klouz, V., Fierro, V., Denton, P., et al., Ethanol reforming for hydrogen in a hybrid electric vehicle: process optimization, *J. Power Sources*, 2002, vol. 105, p. 26.
50. Bergamaschi, V.S., Carvalho, F.M.S., Rodrigues, C., and Fernandes, D.B., Preparation and evaluation of zirconia microspheres as inorganic exchanger in adsorption of copper and nickel ions and as catalyst in hydrogen production from bioethanol, *Chem. Eng. J.,* 2005, vol. 112, p. 153.
51. Meshcheryakov, V.D. and Kirillov, V.A., Thermodynamic equilibrium in the synthesis of dimethyl ether from synthesis gas, *Theor. Found. Chem. Eng.*, 2000, vol. 34, p. 85.
52. Kirillov V.A., Meshcheryakov V.D., Sobyanin V.A., et al., Bioethanol as a promising fuel for fuel cell power plants, *Theor. Found. Chem. Eng.*, 2008, vol. 42, p.1.
53. Pino, L., Vito, A., Cipiti, F., et al., Hydrogen production by methane tri-reforming process over Ni–ceria catalysts: effect of La-doping, *Appl. Catal., B*, 2011, vol. 104, p. 64.
54. Song, C. and Pan, W., Tri-reforming of methane: a novel concept for catalytic production of industrially useful synthesis gas with desired H_2/CO ratios, *Catal. Today*, 2004, vol. 98, p. 463.
55. Kang, J.S., Kim, D.H., Lee, S.D., et al., Nickel-based tri-reforming catalyst for the production of synthesis gas, *Appl. Catal., A*, 2007, vol. 332, p. 153.
56. Jiang, H., Li, H., and Yi, Z., Tri-reforming of methane to syngas over Ni/Al_2O_3—thermal distribution in the catalyst bed, *J. Fuel Chem. Technol.*, 2007, vol. 35, p. 72.
57. Jiang, H., Li, H., Xu, H., and Zhang, Y., Preparation of $Ni/Mg_xTi_{1-x}O$ catalysts and investigation on their stability in tri-reforming of methane, *Fuel Process. Technol.*, 2007, vol. 88, p. 988.
58. Aboosadi, Z.A., Jahanmiri, A.H., and Rahimpour, M.R., Optimization of tri-reformer reactor to produce synthesis gas for methanol production using differential evolution method, *Appl. Energy*, 2011, vol. 88, p. 2691.
59. Reed, R., Prausnits, J., and Sherwood, T., *Properties of Gases and Liquids*, New York: McGraw-Hill, 1977.
60. Kirillov, V.A., Kuzin, N.A., Amosov, Yu.I., et al., Catalysts for the conversion of hydrocarbon and synthetic fuels for onboard syngas generators, *Cat. Ind.*, 2011, no. 2, p. 176.
61. Brizitskii, O.F., Terent'ev, V.Ya., Khristolyubov, A.P., et al., RF Patent 2350839, *Byull. Izobret.*, 2009, no. 9.
62. Sahoo, D.R., Vajpai, S., Sanjay, P., and Pant, K.K., Kinetic modeling of steam reforming of ethanol for the production of hydrogen over Co/Al_2O_3 catalyst, *Chem. Eng. J.*, 2007, vol. 125, p. 139.
63. Peppley, B., Amphlett, J.C., Kearns, L.M., and Mann, R.F., Methanol-steam reforming on $Cu/Zn/Al_2O_3$ catalysts. Part 2: A comprehensive kinetic model, *Appl. Catal., A*, 1999, vol. 179, p. 31.
64. Kirillov V.A., Kuzin N.A., Kuz'min V.A., et al., Radial reactor–heat exchanger for natural gas combustion in a structured porous metal catalyst bed, *Theor. Found. Chem. Eng.*, 2005, vol. 39, p. 407.
65. Kirillov V.A., Kuzin N.A., Kulikov A.V., et al., Thermally coupled catalytic reactor for steam reforming of methane and liquid hydrocarbons: experiment and mathematical modeling, *Theor. Found. Chem. Eng.*, 2003, vol. 37, p. 276.
66. Kirillov V.A., Kuzin N.A., Kireenkov V.V., et al., Use of syngas as an auto fuel additive: state of the art and prospects, *Theor. Found. Chem. Eng.*, 2011, vol. 45, p. 127.
67. Fomin, V.M. and Atrash, R., Improvement of operating parameters of a diesel engine powered by a binary biocarbon fuel, *Transp. Altern. Topl.*, 2012, no. 5, p. 53.

Translated by E. Glushachenkova